International Journal of Nanomedicine

Dovepress
Taylor & Francis Group

Open Access Full Text Article

ORIGINAL RESEARCH

Engineered Exosomes Co-Delivering EGF and FGF Ameliorate Androgenetic Alopecia in a Mouse Model

Yongxian Lai[1–3,*], Junchao Wu[2,4,*], Tianhao Tan[4], Bo Gao[5], Jie Han[2,3], Zhongmin Liu[2,4], Xiaofeng Ding[1,2]

[1]Shanghai Skin Disease Hospital, School of Medicine, Tongji University, Shanghai, People's Republic of China; [2]Shanghai Institute of Stem Cell Research and Clinical Translation, Shanghai, People's Republic of China; [3]School of Pharmacy, Nanjing University of Chinese Medicine, Nanjing, People's Republic of China; [4]Shanghai East Hospital, School of Medicine, Tongji University, Shanghai, People's Republic of China; [5]Umibio (Shanghai) Co. Ltd, Shanghai, People's Republic of China

*These authors contributed equally to this work

Correspondence: Xiaofeng Ding, Shanghai Skin Disease Hospital, School of Medicine, Tongji University, Shanghai, 200443, People's Republic of China, Email dingxiaofeng1993@163.com; Zhongmin Liu, Shanghai East Hospital, School of Medicine, Tongji University, Shanghai, 200120, People's Republic of China, Email zhongminliu01@gmail.com

Background: Androgenetic alopecia (AGA) is characterized by hair follicle miniaturization and growth factor deficiency. However, conventional therapies such as minoxidil and finasteride fail to restore the pathological follicular microenvironment, highlighting the urgent need for novel therapeutic strategies. Epidermal growth factor (EGF) and fibroblast growth factor (FGF) are key regulators of hair follicle regeneration, yet their expression is downregulated in the follicular microenvironment of AGA patients.

Methods: This study validated the expression profile of growth factors in hair follicles of AGA patients through clinical sample analysis. Subsequently, dual-factor engineered exosomes (EXO-EGF/FGF) loaded with EGF and FGF were constructed using LAMP2B fusion engineering technology with 293T cells as donor cells. EXO-EGF/FGF was characterized by transmission electron microscopy (TEM) and nanoparticle tracking analysis (NTA). The regulatory effects of EXO-EGF/FGF on human dermal papilla cells (HDPCs) were evaluated in vitro. An androgen-induced AGA mouse model was established to assess the therapeutic efficacy and safety of EXO-EGF/FGF in vivo.

Results: Clinical sample analysis confirmed that the expression of EGF and FGF was significantly downregulated in dermal papilla cells of AGA patients, leading to reduced expression of NOTCH signaling pathway proteins associated with hair follicle regeneration. TEM and NTA results demonstrated that EXO-EGF/FGF exhibited exosomal morphology, with significantly higher expression levels of EGF and FGF than natural exosomes. In vitro experiments revealed that EXO-EGF/FGF promoted the proliferation and migration of HDPCs by reactivating the cell cycle and enhancing migration-related programs. In the AGA mouse model, EXO-EGF/FGF effectively restored hair coverage density and follicular structural integrity without inducing immunogenic reactions or systemic toxicity, and significantly increased the number of anagen-phase hair follicles in post-treatment tissues.

Conclusion: This study demonstrated that LAMP2B-engineered EXO-EGF/FGF acted on follicular cells to repair the pathological microenvironment in AGA. This strategy overcame the inherent limitations of conventional therapies and natural exosomes, offering a novel, safe, and clinically translatable therapeutic approach for AGA treatment.

Keywords: androgenetic alopecia, engineered exosomes, growth factor, follicular microenvironment, clinical translation

Introduction

Androgenetic alopecia (AGA) was the most prevalent form of hair loss globally, characterized by follicular miniaturization and disruption of the hair growth cycle.[1,2] The Hamilton-Norwood classification system categorized male AGA severity into stages I through VII.[3] Epidemiological studies revealed that the prevalence of AGA among men aged 30–50 reached 58%, with progression observed alongside aging. By the age of 70, over 80% of Caucasian males and approximately 50% of Caucasian females had been affected.[3] In Asian populations, 41.4% of Chinese men and 11.8% of Chinese women would

https://doi.org/10.2147/IJN.S572518
Received: 7 October 2025
Accepted: 6 February 2026
Published: 16 February 2026

Graphical Abstract

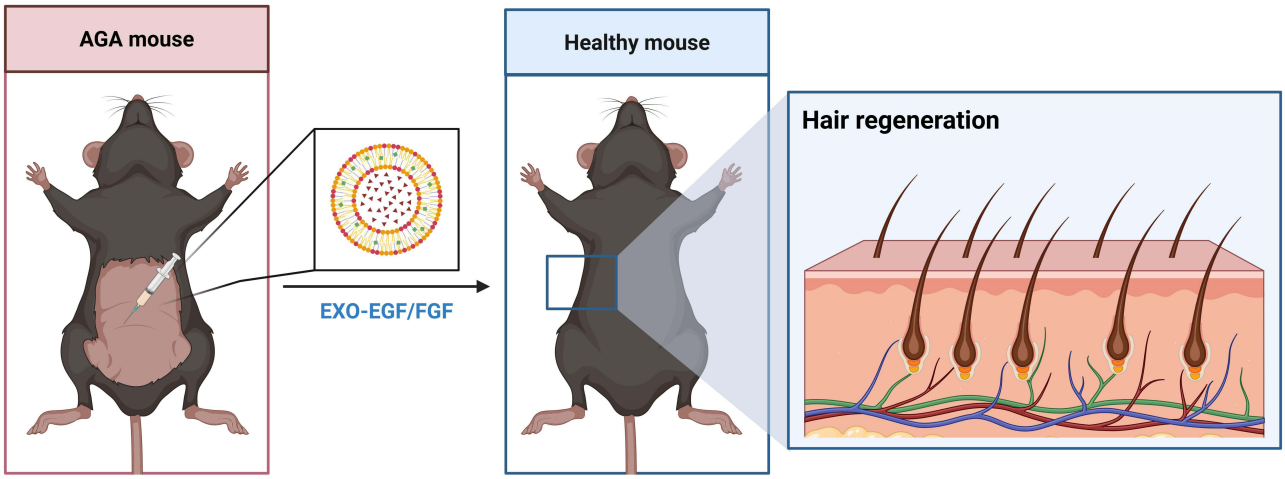

develop AGA within the same age range.[4] The pathogenesis of AGA resulted from the synergistic effects of multiple factors, involving genetic and epigenetic regulation, imbalances in androgen metabolism, immune-inflammatory responses, oxidative stress, and dysregulation of key signaling pathways such as Wnt/β-catenin, BMP, and Notch.[5]

However, current first-line clinical treatments for AGA, minoxidil and finasteride, exhibited significant limitations. Minoxidil required long-term administration due to its low transdermal efficiency and carried a high risk of relapse upon discontinuation.[6] Finasteride might induce sexual function-related side effects and failed to reverse already atrophied follicular structures.[7] Although low-level laser therapy (600–950 nm) could improve hair parameters, it similarly could not restore miniaturized follicles.[8] Hair transplantation surgery was constrained by the limited availability of donor follicles and its inability to remodel the pathological microenvironment in balding areas, making it insufficient for severe AGA cases.[9] Consequently, there is an urgent need to develop novel therapies capable of synergistically regulating the multi-pathway networks involved in follicular regeneration.

Studies revealed reduced expression of key factors including FGF, VEGF, and IGF-1 in the telogen-phase follicles of AGA patients.[10] Epidermal Growth Factor (EGF) and Fibroblast Growth Factor (FGF) played pivotal roles in dynamically regulating hair follicle regeneration. Specifically, FGF9 was found to promote β-catenin nuclear translocation by activating the FGFR3-ERK1/2 pathway, thereby driving de novo hair follicle formation in murine models.[11] EGF demonstrated direct interaction with the Notch signaling pathway.[12,13] Low concentrations (2–20 ng/mL) of EGF were shown to induce release of the Notch intracellular domain via a γ-secretase-dependent mechanism, upregulating Notch1/Jagged1 expression and downstream target genes Hes1/Hes5, consequently maintaining follicular stem cell pluripotency and driving cell cycle progression.[14] Clinical investigations confirmed that autologous platelet-rich plasma, through supplementation of EGF and FGF-2 among other factors, effectively stimulated human follicular dermal cell proliferation and prolonged the anagen phase.[10] Consequently, the synergistic action of FGF and EGF regulates the proliferation, differentiation, and survival of human dermal papilla cells (HDPCs) and follicular epithelial cells, offering a potential therapeutic approach for the multi-pathway dysregulation observed in AGA.

However, the topical application of free EGF/FGF had limited therapeutic efficacy. On the one hand, the physical barrier formed by the stratum corneum prevented the penetration of high-molecular-weight growth factors, restricting their access to follicular targets in the dermis.[15] On the other hand, proteases in the scalp microenvironment rapidly degraded these free factors, shortening their half-life and making it difficult to maintain effective local therapeutic concentrations.[16] Besides, the lack of targeting specificity in free factors led to their diffusion into surrounding non-target tissues, thereby reducing local bioavailability.[17] Therefore, the therapeutic application of EGF/FGF for AGA required both efficient targeted delivery and sustained maintenance of effective local concentrations.

Exosomes served as nanoscale messengers in intercellular communication, emerging as a research focus in regenerative medicine due to their innate drug-loading capacity, low immunogenicity, and microenvironment-modulating properties.[18] Multiple exosome-based therapies had demonstrated therapeutic potential. Naturally derived exosomes, including those isolated from platelet-rich plasma and mesenchymal stem cells, were verified to promote hair follicle development and enhance hair density through upregulation of VEGF signaling pathways.[19–21] However, naturally derived exosomes presented inherent limitations.[22] Their endogenous growth factor content was low, insufficient to sustainably activate regenerative pathways.[22] And naturally derived exosomes lacked follicle-targeting specificity, being readily taken up by non-target cells.[22,23] Engineered exosomes, such as fisetin-treated human keratinocyte-derived exosomes, were shown to prolong the anagen phase via antioxidative stress mechanisms.[24] However, the efficacy of these exosomes was constrained by insufficient growth factor content, failing to sustainably activate follicular regeneration pathways. To address these limitations, this study employed LAMP2B fusion technology.[25] Lysosome-associated membrane protein 2B (LAMP2B) is an exosomal surface marker whose transmembrane domain anchors to the exosomal lipid bilayer.[25] By fusing EGF/FGF to the C-terminus of LAMP2B, the growth factors were directly loaded onto the exosomal membrane surface.[25] Through LAMP2B-mediated cellular uptake, this design significantly enhanced the stability and delivery efficiency of the therapeutic molecules to target cells.[26]

Based on this foundation, this study employed gene-editing technology to construct engineered exosomes overexpressing EGF and FGF via LAMP2B fusion engineering in 293T cells (EXO-EGF/FGF). These engineered exosomes exhibited higher EGF/FGF loading capacity than natural exosomes. In vitro experiments demonstrated that EXO-EGF/FGF significantly promoted the proliferation, migration, and regeneration of HDPCs. In AGA mice model, local injection of EXO-EGF/FGF enhanced hair regeneration, with treated animals showing improved hair density and coverage compared to controls. Histological analysis demonstrated an increased number of anagen-phase hair follicles. These findings confirmed that EXO-EGF/FGF provided an efficient and long-lasting novel paradigm for AGA therapy.

Materials and Methods

Plasmid Construction and Transfection

The construction of Lamp2b-based fusion plasmids was performed to generate exosomes overexpressing EGF, FGF, or a combination of both (FGF-EGF). The pcDNA3.1 vector was selected as the backbone for cloning. Three distinct plasmids were engineered: (1) pcDNA3.1-SP-EGF-LAMP2B, (2) pcDNA3.1-SP-FGF-LAMP2B, and (3) pcDNA3.1-SP-FGF-EGF-LAMP2B. The pcDNA3.1 vector was utilized as the backbone, into which human EGF (UniProt ID: P01133), FGF (UniProt ID: P05230), or a dual FGF-EGF sequence was inserted and fused with the transmembrane domain of Lamp2b (UniProt ID: P13473-2). Each construct was driven by the CMV promoter and incorporated an N-terminal signal peptide (MVCFRLFPVPGSGLVLVCLVLGAVRSYA) to ensure precise localization of the fusion proteins onto exosomal membranes. Following directional cloning via BamHI/EcoRI restriction digestion, plasmid sequences were confirmed by Sanger sequencing. For transfection, 293T cells were seeded at 2×10^6 cells per dish in serum-free medium and co-transfected with 8 μg of target plasmid, 6 μg psPAX, and 4 μg pMD using Lipofectamine 2000. The culture supernatant was harvested 72 hours post-transfection for exosome isolation.

Experimental Materials

Antibodies for β-actin (#AC026), Ki67 (#A20018), EGF (#A26211), FGF (#A26623PM), and HRP-conjugated Goat anti-Rabbit IgG (H+L) (#AS014) were purchased from Wuhan ABclonal Biotechnology Co., Ltd. The EGF antibody (#M805) was purchased from Thermo Fisher Scientific. The CCK-8 assay kit (#C0038), cell cycle detection kit (#C1052), BCA protein quantification kit (#P0398M), RIPA lysis buffer (#P0013B), and PMSF (#ST505) were purchased from Beyotime Biotechnology (Shanghai, China). Dihydrotestosterone (DHT, #PA86447) was purchased from Perfemiker Chemical Technology Co., Ltd. (Shanghai, China). The PAGE gel rapid preparation kit (#PG112) and dual-color pre-stained protein marker (#WJ103) were purchased from Epizyme Biotech Co., Ltd. (Shanghai, China).

Cell and Animal Culture

HDPCs and HEK293T cells were purchased from Merck Group. The cells were cultured in high-glucose DMEM medium supplemented with 10% fetal bovine serum (FBS) and 1% penicillin/streptomycin and maintained at 37°C under 5% CO_2 atmosphere. Male C57BL/6 mice aged 6–8 weeks, provided by SPF Biotechnology Co., Ltd., were housed in a pathogen-free environment.

Human scalp sample collection was approved by the Institutional Review Board of BGI (Approval No.: BGI-IRB 22047-T1) and the Ethics Committee of Shanghai Skin Disease Hospital (Approval No.: 2023–45), and all procedures complied with the principles of the Declaration of Helsinki, with written informed consent obtained from all donors prior to sample collection. Three AGA samples were selected from 11 enrolled adults. The AGA donors were aged 38–45 years and consisted of 2 males and 1 female, with the males classified as Hamilton-Norwood stage III–IV and the female classified as Ludwig stage II. Three healthy control (HC) samples were obtained from 90 volunteers, and the HC donors were age-matched with the AGA group and included 1 male and 2 females, all with no clinical evidence of hair loss or scalp diseases. All donors met the following inclusion and exclusion criteria. They were 20–59 years old and had no history of severe systemic diseases. Among them, AGA donors were clearly diagnosed by dermatologists, and HC donors had normal hair status confirmed by trichoscopy. The exclusion criteria included presence of scalp or other skin disorders, self-reported pregnancy or lactation, use of topical or systemic anti-hair loss drugs or immunosuppressants within 3 months prior to sample collection, and failure to provide informed consent. The 10 mm × 10 mm scalp samples were dissected from donors at the Department of Dermatologic Surgery, Shanghai Skin Disease Hospital, under local anesthesia to ensure the safety and comfort of donors during the collection process.

Exosome Preparation and Characterization

The recombinant plasmid constructed previously was transfected into HEK293T cells using Lipofectamine 2000 transfection reagent. Six-hour post-transfection, the medium was replaced with DMEM complete medium containing exosome-depleted fetal bovine serum (FBS), followed by further incubation for 48–72 hours. The conditioned medium was collected and purified through multiple centrifugation steps: centrifugation at 500 × g for 10 minutes to remove cells, at 2000 × g for 10 minutes to eliminate large debris, and at 10,000 × g for 30 minutes to pellet large vesicles. The supernatant was filtered through a 0.22 μm PES membrane filter, and exosomes were precipitated via ultracentrifugation (140,000 × g, 2 hours, 4°C). The resulting exosome pellet was resuspended in PBS storage buffer and stored at −80°C for future use.

Subsequently, the morphology of exosomes was observed using transmission electron microscopy (TEM), their size distribution was determined by nanoparticle tracking analysis (NTA), their concentration was performed using nano-flow cytometry, and the expression of the Lamp2b fusion protein was detected by SDS-PAGE.

Cell Viability Detection

The CCK-8 assay was used to evaluate the effect of EXO-EGF/FGF on the viability of HDPCs. HDPCs were seeded in a 96-well plate and pretreated with 1 mM/L DHT for 24 hours. Subsequently, complete medium containing varying concentrations of EXO-EGF/FGF (0–320 μg/mL) was added and incubated for another 24 hours. Then, 10 μL of CCK-8 solution was added to each well and reacted for 2 hours. The absorbance at 450 nm was measured using a microplate reader, and the percentage of cell survival rate was calculated with the untreated group as the control.

Proliferation Cycle Detection

A cell cycle detection kit was used to evaluate the effect of EXO-EGF/FGF on HDP proliferation. HDPCs were seeded in a 6-well plate and pretreated with 1 mM/L DHT for 24 hours. After treatment with EXO-EGF/FGF for 24 hours, the cells were digested with trypsin, centrifuged, and washed. They were then fixed with 70% ethanol at 4°C. According to the kit instructions, propidium iodide (PI) staining solution (containing RNase A) was prepared, and the cells were stained in the dark for 30 minutes. Fluorescence signals were detected using a Navios 6 COLORS/2 LASER flow cytometer, and cell cycle distribution was analyzed with FlowJo Software.

Scratch Assay

A cell scratch assay was used to evaluate the effect of EXO-EGF/FGF on the migration ability of HDPCs. HDPCs were seeded in a 6-well plate and pretreated with 1 mM/L DHT for 24 hours. After reaching 90% confluency, the monolayer was scratched using a 200 μL pipette tip. The cells were then washed with PBS and treated with 160 μg/mL EXO-EGF /FGF. Images of the cells in the plate were captured at different time points using an optical microscope. The percentage of wound closure was calculated using ImageJ software.

Establishment and Treatment of AGA Animal Model

Eighteen 7-week-old male C57BL/6J mice were used to construct AGA models. After removing telogen-phase hair from a 2 cm × 3 cm dorsal area using depilatory cream, the mice were randomly divided into three groups, control group (injected with EXO-NC, labeled as EXO-NC), model group (topically administered testosterone propionate and injected with EXO-NC, labeled as EXO-NC + DHT), and treatment group (topically administered testosterone propionate and injected with EXO-EGF/FGF, labeled as EXO-EGF/FGF + DHT). From Day 0 to Day 12, the model and treatment groups received daily topical application of 200 μL of 0.5% w/v testosterone solution (dissolved in 50% v/v ethanol solution) to establish the AGA model.[27] Starting from Day 1, the treatment group received subcutaneous injections of EXO-EGF/FGF every other day. Hair growth in each group was observed and recorded every 4 days, and the animal experiment was terminated on Day 12. Hair regeneration was monitored and quantified at specific time points using Image J software.

Histological and Immunohistochemical Analysis

On day 12 of treatment, skin samples from all mice along with liver, spleen, and kidney specimens were collected and fixed in 4% paraformaldehyde solution. The fixed tissues and organs underwent sequential gradient ethanol dehydration, xylene clearing, and paraffin embedding. Subsequently, the embedded tissues were subjected to hematoxylin–eosin (HE) staining and immunohistochemical analysis.

For HE staining, 5 μm sections were stained with hematoxylin and counterstained with eosin, followed by mounting. For immunohistochemistry, 5 μm sections underwent antigen retrieval and blocking, followed by incubation with primary antibodies against EGF (1:1000), FGF (1:1000), and Ki67 (1:1000). Finally, Anti-Rabbit IgG (H+L) HRP Affinity Purified Polyclonal Antibody (1:200) was added and incubated for 1 hour, followed by DAB staining and mounting. All images were observed and captured using an inverted fluorescence microscope.

Western Blot Analysis

Skin tissue samples (20 mg) and exosomes samples were homogenized using an electric homogenizer (Jingxin, China) in RIPA lysis buffer containing 1% PMSF, followed by centrifugation at 12,000 rpm for 20 minutes. Protein concentration was determined using a BCA protein quantification kit. Then, 20 μg of protein samples were separated by 10% SDS-PAGE electrophoresis and transferred to a nitrocellulose membrane. The membranes were incubated with primary antibodies against Ki67 (1:1000), EGF (1:1000), and FGF (1:2000), respectively. Detection was performed using HRP-conjugated secondary antibodies (1:1000), and signals were captured with a chemiluminescence imaging system.

Statistical Analysis

All experimental data are presented as mean ± standard deviation (Mean ± SD). Unless otherwise specified, all experiments were performed with three biological replicates. Differences between groups were analyzed using one-way analysis of variance (one-way ANOVA), with multiple comparisons conducted by Tukey's post-hoc test. Comparisons between two groups were performed using Student's *t*-test. Statistical significance was indicated by $*P < 0.05$, highly significant by $**P < 0.01$, and extremely significant by $***P < 0.001$. All statistical analyses were performed using GraphPad Prism 9.0 software.

Results

Deficiency of Hair EGF/FGF Expression in AGA Patients

Single-cell RNA sequencing (scRNA-seq) was performed on hair follicle cells from scalp tissues of three AGA patients and three HC. Uniform manifold approximation and projection analysis identified 15 distinct cell clusters, revealing significant downregulation of NOTCH pathway genes (P <0.05) in hair medulla, cortex, and inner root sheath cells (Figure 1A). Given that the NOTCH signaling pathway acts as a key downstream effector of EGF/FGF and functionally depends on growth factor activation, this downregulation strongly suggests potential EGF/FGF expression impairment in AGA hair follicles.[14,28] This hypothesis was subsequently confirmed via immunofluorescence co-localization, with EGF and FGF deficiencies primarily localized to the dermal papilla and outer root sheath (Figure 1B). Western blot and semi-quantitative results further demonstrated significantly reduced EGF and FGF protein levels in AGA hair follicles compared to HC ($P < 0.05$) (Figure 1C). Consistently, immunohistochemistry analysis of scalp tissue sections showed reduction in both EGF and FGF protein expression within the hair follicles of AGA patients compared to those from HCs (Figure 1D).

Isolation and Characterization of EXO-EGF/FGF

To achieve targeted delivery of EGF and FGF to hair follicles, this study constructed 293T-derived exosomes expressing an EGF-FGF fusion protein. The coding sequences of EGF and FGF2 were tandemly linked via a flexible glycine-serine connector and further fused to the N-terminus of the exosomal membrane protein LAMP2B. This fusion expression cassette was cloned into a CMV promoter-driven pcDNA3.1(+) vector (Figure 2A). Stable transfected cell lines were obtained through G418 screening (800 μg/mL, 14 days), and exosomes were isolated from the conditioned medium by differential ultracentrifugation.

Subsequent systematic characterization confirmed the successful preparation of functional exosomes EXO-EGF/FGF. TEM revealed that EXO-EGF/FGF exhibited a typical cup-shaped double-membrane vesicular structure (Figure 2B). NTA demonstrated a homogeneous size distribution with a peak diameter of 98 nm and a particle concentration of 2.69×10^{11} particles/mL, consistent with exosomal characteristics (Figure 2C and D). Zeta potential analysis indicated moderate stability of EXO-EGF/FGF (Figure 2E). SDS-PAGE further confirmed that EXO-EGF/FGF shared characteristic protein profiles with 293T exosomes (EXO-NC), with specific enrichment of EGF and FGF proteins and significantly elevated expression levels compared to 293T exosomes (Figure 2F). Subsequently, specific bands corresponding to the EGF-FGF fusion protein were detected in EXO-EGF/FGF samples using anti-EGF and anti-FGF2 antibodies, while no corresponding bands were observed in the control exosome samples, confirming the successful loading of the target protein ($P < 0.001$) (Figure 2G).

To assess potential cytotoxicity, an AGA cell model was established using DHT-induced HFDPCs. After treatment with gradient concentrations of EXO-EGF/FGF (0–320 μg/mL) for 24 hours, CCK-8 results showed significantly enhanced cell viability at all tested concentrations, confirming that EXO-EGF/FGF lacks cytotoxicity and promotes cell proliferation ($P > 0.05$ versus untreated control group) (Figure 2H). Furthermore, since the 160 μg/mL concentration of EXO-EGF/FGF exhibited the optimal cell proliferation-promoting effect, this concentration was selected for subsequent experiments.

In vitro Promotion of Hair Follicle Regeneration

To investigate the therapeutic mechanism of EXO-EGF/FGF against AGA, AGA cell models were established by pretreating HFDPCs with testosterone propionate for 24 hours. The model was subsequently treated with either EXO-NC or EXO-EGF/FGF. Flow cytometry analysis revealed that intervention with 160 μg/mL EXO-EGF/FGF induced significant cell cycle redistribution in HFDPCs. Specifically, after EXO-EGF/FGF treatment, the proportion of cells in the G0/G1 phase decreased from 69.5% to 53.2% ($P < 0.05$), while the S phase population increased from 18.9% to 34.2% ($P < 0.05$), and the G2/M phase proportion rose from 11.1% to 12.0% ($P < 0.05$) (Figure 3A). This shift demonstrated that EXO-EGF/FGF drives cell proliferation by promoting G1/S phase transition, effectively reprogramming the cell cycle of HFDPCs.

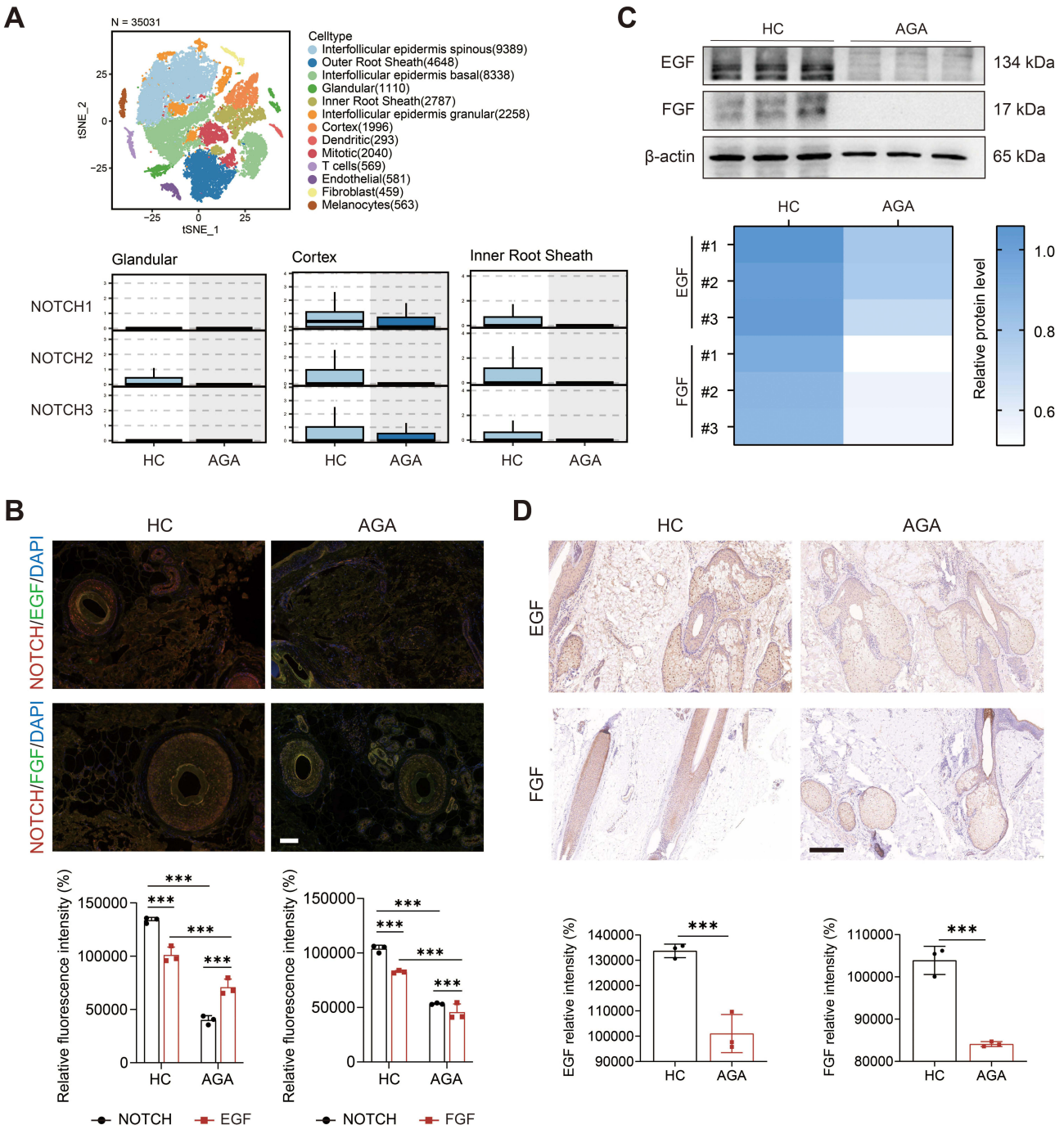

Figure 1 Downregulation of NOTCH pathway and growth factors in AGA hair follicles. (**A**) scRNA-seq revealed downregulation of NOTCH, EGF, and FGF expression in the medulla, cortex, and inner root sheath of AGA hair follicles. (**B**) Immunofluorescence confirms reduced NOTCH and EGF/FGF levels in AGA hair follicles. Red: NOTCH. Green: EGF/FGF. Blue: DAPI Scale bar = 50 μm. (**C**) Western blot demonstrated decreased EGF/FGF protein expression in AGA hair tissue compared to HC. (**D**) Immunohistochemistry staining demonstrated diminished expression levels of EGF and FGF proteins in AGA hair follicles. Scale bar = 200 μm. Data were expressed as mean ± SD (n = 3 for each group). ***$P < 0.001$.

Ki67 immunofluorescence staining further confirmed the proliferative enhancement induced by EXO-EGF/FGF. The fluorescence intensity in healthy HFDPCs controls was 16.7%, whereas EXO-EGF/FGF intervention in the AGA model markedly increased nuclear Ki67 signals, with fluorescence intensity rising from 3.4% to 47.4% ($P < 0.05$) (Figure 3B).

Scratch assay results quantified the migratory capacity of HFDPCs toward wounded areas. Measurement of wound closure rates at 12, 24, and 48 hours post-treatment showed that after 48 hours, the healthy HFDPCs control group

https://doi.org/10.2147/IJN.S572518

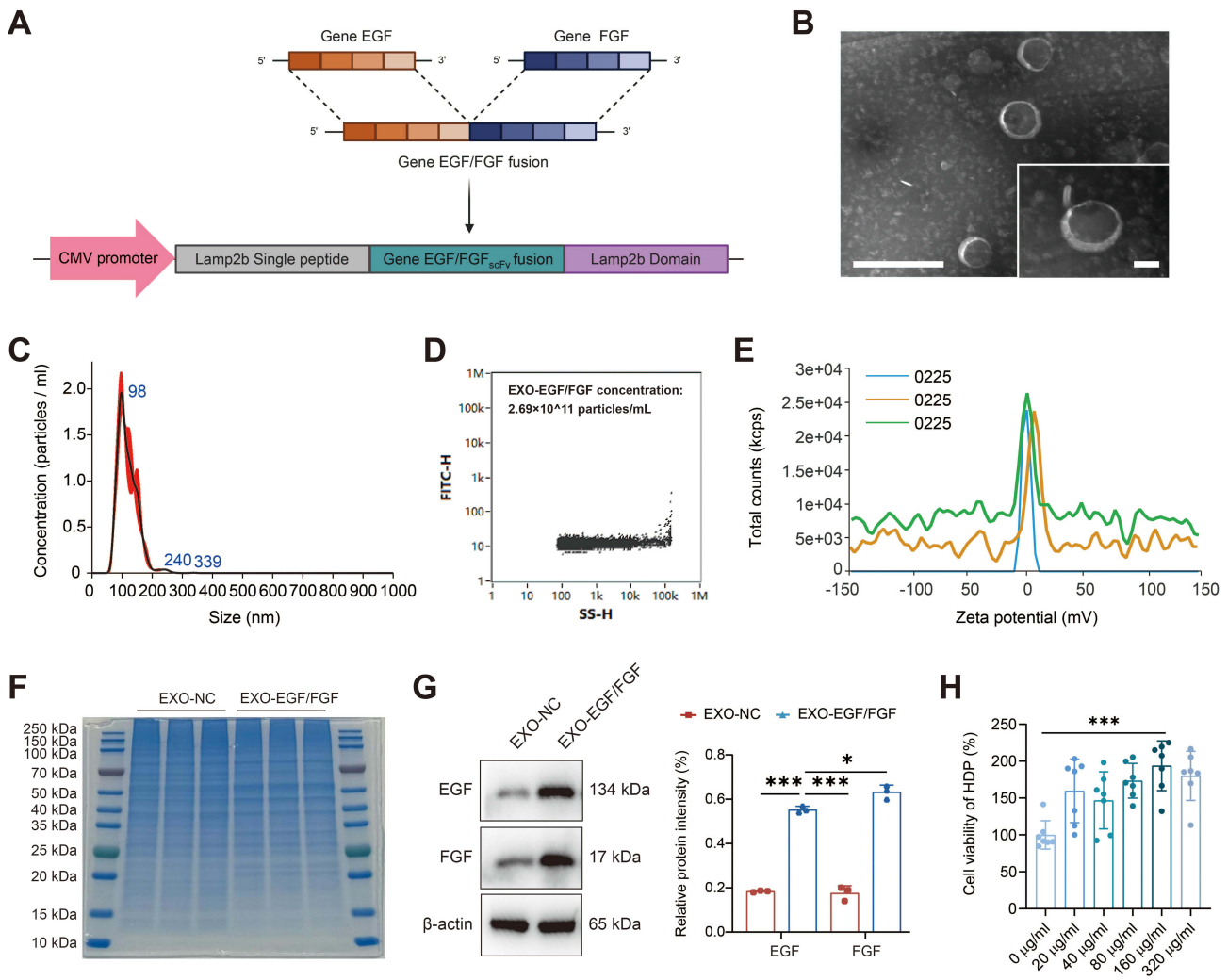

Figure 2 Construction and characterization of EXO-EGF/FGF. (**A**) Schematic design of the EGF-FGF-LAMP2B fusion protein. (**B**) TEM images showed the typical vesicular morphology of EXO-EGF/FGF. Scale bar = 100 nm. (**C**) NTA confirmed the particle size distribution of EXO-EGF/FGF within the range of 90–120 nm. (**D**) Nano-flow cytometry confirmed the particle concentration of EXO-EGF/FGF. (**E**) Zeta potential analysis indicated a surface charge of approximately −25 mV for EXO-EGF/FGF (n = 3). (**F**) SDS-PAGE revealed a specific band at 75 kDa in the EXO-EGF/FGF group. (**G**) Western blot analysis of the EGF and FGF protein expression in exosomes. (**H**) CCK-8 assay demonstrated enhanced viability of HFDPCs after 24-hour treatment with EXO-EGF/FGF (n = 7). **P* < 0.05, ***P* < 0.01, ****P* < 0.001.

achieved 38.7% closure, while the AGA model group reached 35.8%. In contrast, EXO-EGF/FGF treatment significantly enhanced wound closure in the AGA model to 65.6%, exhibiting a statistically significant difference compared to the untreated AGA model group ($P < 0.05$) (Figure 3C). These results indicated that EXO-EGF/FGF effectively promoted cell proliferation, migration, and cell cycle progression in AGA models.

EXO-EGF/FGF Promoted Hair Regeneration in AGA Animal Models

To evaluate the therapeutic efficacy of EXO-EGF/FGF, three experimental groups were established: the normal hair loss control group receiving mechanical depilation with bi-daily injections of 100 μL EXO-NC, the AGA model group subjected to topical 0.5% testosterone application, and the EXO-EGF/FGF treatment group undergoing AGA induction via testosterone followed by bi-daily 100 μL EXO-EGF/FGF injections (Figure 4A). After 12 days, hair growth assessment revealed that normal hair loss mice exhibited robust spontaneous regeneration with 82.7% hair coverage, while AGA models maintained alopecic patches at 21.5% coverage ($P < 0.05$ versus control). Notably, EXO-EGF/FGF treatment reversed androgen-induced hair loss, restoring density to near-normal levels (58.4% coverage) (Figure 4B and C).

https://doi.org/10.2147/IJN.S572518

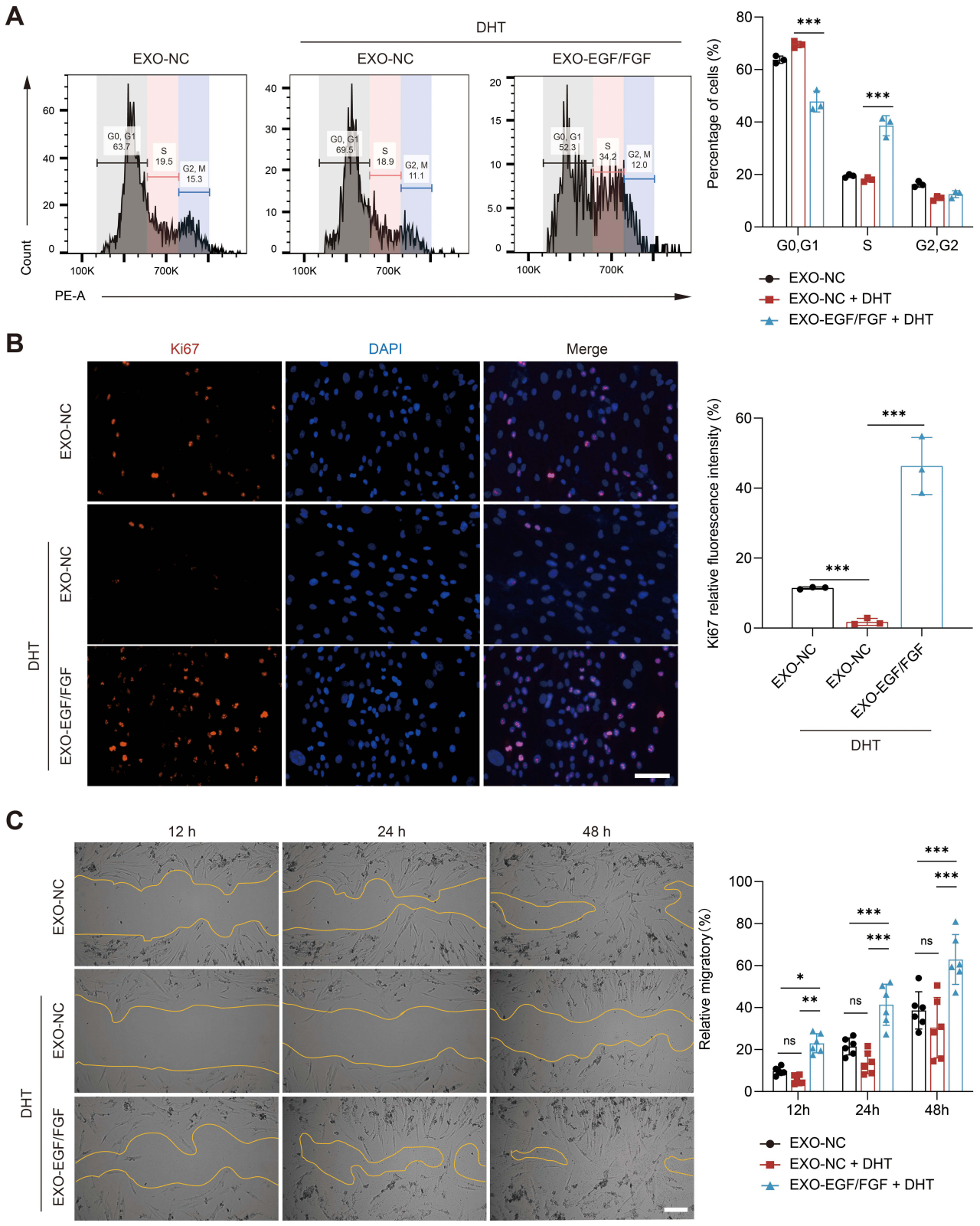

Figure 3 EXO-EGF/FGF promotes proliferation and migration of HFDPCs. (**A**) Flow cytometry analysis demonstrated that EXO-EGF/FGF facilitated G1/S phase transition in HFDPCs (n = 3). (**B**) Ki67 immunofluorescence staining showed EXO-EGF/FGF enhanced proliferation of HFDPCs (n = 3). Scale bar = 50 μm. Red: Ki67. Blue: DAPI. (**C**) Scratch assay at 12, 24, and 48 hours confirmed EXO-EGF/FGF-induced migration of HFDPCs (n = 6). Scale bar = 200 μm. Ns = no significance, *$P < 0.05$, **$P < 0.01$, ***$P < 0.001$.

https://doi.org/10.2147/IJN.S572518

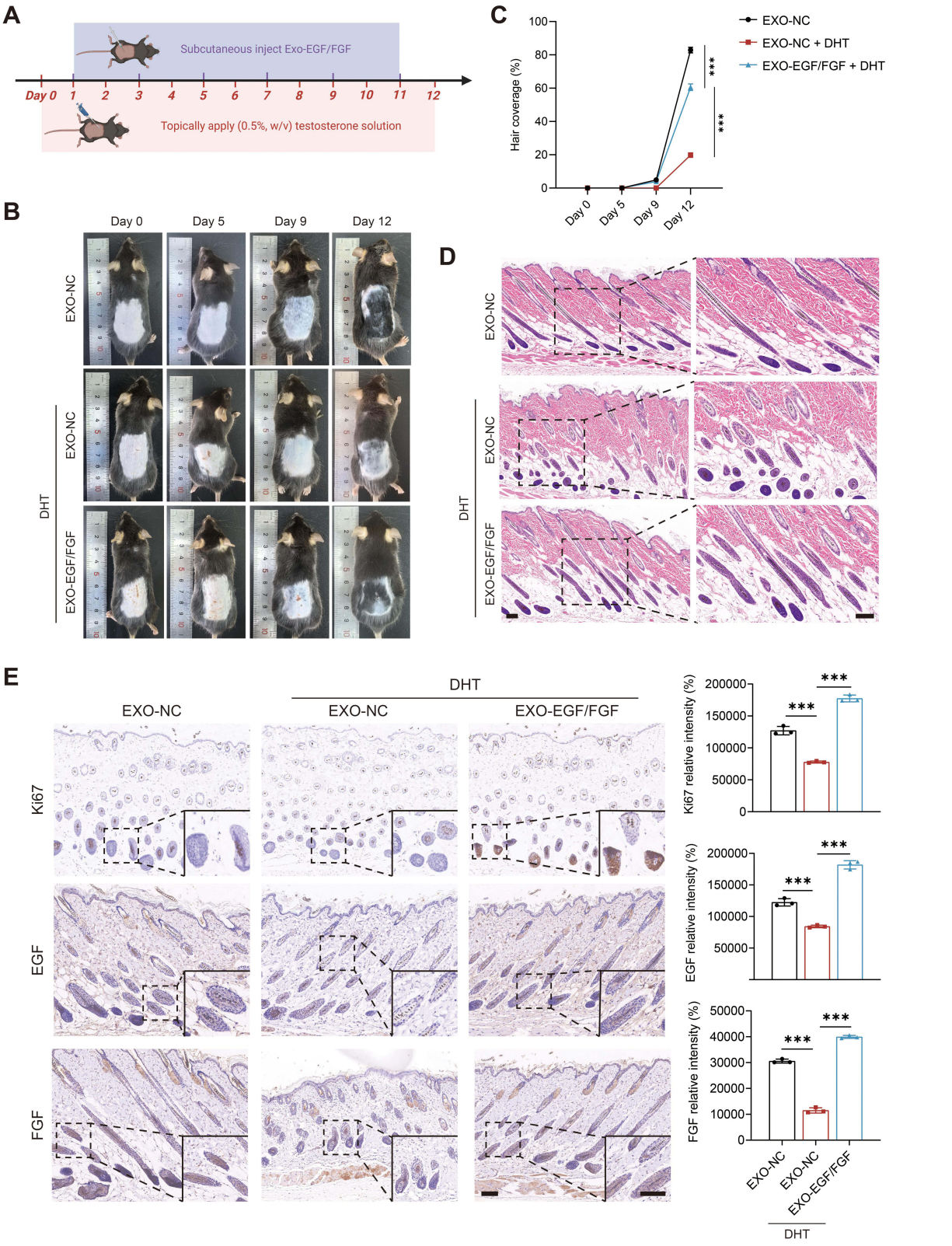

Figure 4 EXO-EGF/FGF promoted hair regeneration in AGA animal models. (**A**) Schematic of the AGA animal model establishment and therapeutic regimen. (**B**) Macroscopic dorsal images demonstrated hair regeneration progress in AGA mice at days 0, 5, 9, and 12. (**C**) Quantification of hair coverage area demonstrated significant improvement in the EXO-EGF/FGF treatment group compared to controls. (**D**) HE staining revealed increased density of anagen-phase hair follicles in the EXO-EGF/FGF-treated group. (**E**) Immunohistochemical analysis confirmed enhanced Ki67/EGF/FGF signaling in the skin of the EXO-EGF/FGF treatment group. Scale bar = 100 μm. ***$P < 0.001$.

https://doi.org/10.2147/IJN.S572518

Histopathological analysis via HE staining demonstrated that control skin contained abundant anagen-phase follicles, whereas AGA tissues were dominated by miniaturized telogen-phase follicles. EXO-EGF/FGF treatment partially restored telogen-to-anagen transition, evidenced by characteristic follicle elongation and melanin deposition (Figure 4D).

Immunohistochemistry further elucidated the mechanistic basis. AGA mice showed significant downregulation of Ki67, EGF, and FGF in hair bulb regions ($P < 0.05$), while EXO-EGF/FGF treatment markedly upregulated these proteins with statistical significance versus AGA group ($P < 0.05$). These results confirm that EXO-EGF/FGF promotes hair regeneration by reversing androgen-driven suppression of proliferation and growth factors, thereby normalizing the pathological hair cycle in AGA.

EXO-EGF/FGF Exhibited in vivo Safety

Following 12-day subcutaneous administration of EXO-EGF/FGF in AGA mice, the biological safety was systematically evaluated. Macroscopic observations revealed intact architectures of major organs (liver, kidneys, heart, lungs, and spleen) in the EXO-EGF/FGF-treated group. Histopathological assessment via HE staining demonstrated absence of pathological lesions, with no observable necrosis, inflammatory infiltration, or fibrotic alterations (Figure 5A).

Complete blood count analysis further confirmed physiological homeostasis, as critical parameters including hemoglobin, white blood cells, and platelets remained within normal ranges (Figure 5B). Hepatic and renal function biomarkers, serum alanine aminotransferase (ALT), aspartate aminotransferase (AST), blood urea nitrogen (BUN), and creatinine levels, all maintained normal physiological ranges (Figure 5C). These collective findings demonstrated that EXO-EGF/FGF possessed favorable biosafety profiles and exhibited translational potential for AGA treatment.

Discussion

AGA is a highly prevalent follicular degenerative disorder, characterized pathologically by progressive follicular miniaturization and shortened anagen phase.[29] To explore the core mechanism of AGA progression and develop targeted therapeutic strategies, this study performed integrated single-cell transcriptomics and proteomics analysis on clinical samples, identifying significant growth factor deficiency in HDPCs of AGA patients. ScRNA-seq data demonstrated marked downregulation of NOTCH gene expression in hair medulla, cortex, and inner root sheath cells ($P< 0.001$) (Figure 1A). Given that NOTCH signaling acts as a key effector downstream of EGF/FGF in regulating follicular stem cell fate, this finding strongly suggests dysfunction in the growth factor cascade.[30] Subsequent comparative analysis with HC revealed through immunofluorescence that the deficient areas exhibited significant colocalization with NOTCH low-expression zones, accompanied by reduced protein levels of EGF and FGF2 (Figure 1B–D). These findings clarified the molecular mechanism about AGA-associated follicular microenvironment disorders and establish a theoretical basis for treating AGA via EGF/FGF supplementation to modulate the follicular microenvironment.

However, conventional AGA therapies failed to overcome delivery barriers and stability limitations, struggling to effectively restore the dysregulated EGF and FGF2 microenvironment in AGA. Although minoxidil, a first-line clinical drug for AGA, could transiently dilate local blood vessels, it suffered from low transdermal absorption rates and an inability to reverse growth factor deficiencies, resulting in high relapse rates after discontinuation.[31] Finasteride similarly exhibited high recurrence rates post-treatment and might cause persistent sexual dysfunction in male patients.[32] Furthermore, finasteride merely blocked androgen conversion pathways without reversing the compromised microenvironment in atrophied hair follicles.[33] It is noteworthy that a comparative clinical study demonstrated that the combination of adipose-derived stem cell secretome, a rich source of multiple growth factors, with minoxidil yielded superior hair regeneration outcomes compared to either monotherapy at the 12-week endpoint, with the most significant improvements observed in terminal hair density and anagen hair ratio.[34] Moreover, the initial telogen effluvium phenomenon observed in the minoxidil-only group was absent in the combination therapy group.[34] This suggested that growth factor therapy may enhance follicular vitality, facilitating a faster and more stable transition through the minoxidil-induced telogen--to-anagen shift phase. These findings corroborated the therapeutic rationale of improving the follicular microenvironment by growth factor supplementation.

To address these unmet clinical needs in AGA treatment, this study constructed an engineered exosome strategy to reconstruct the follicular microenvironment and achieve functional hair regeneration. Through genetic engineering, we

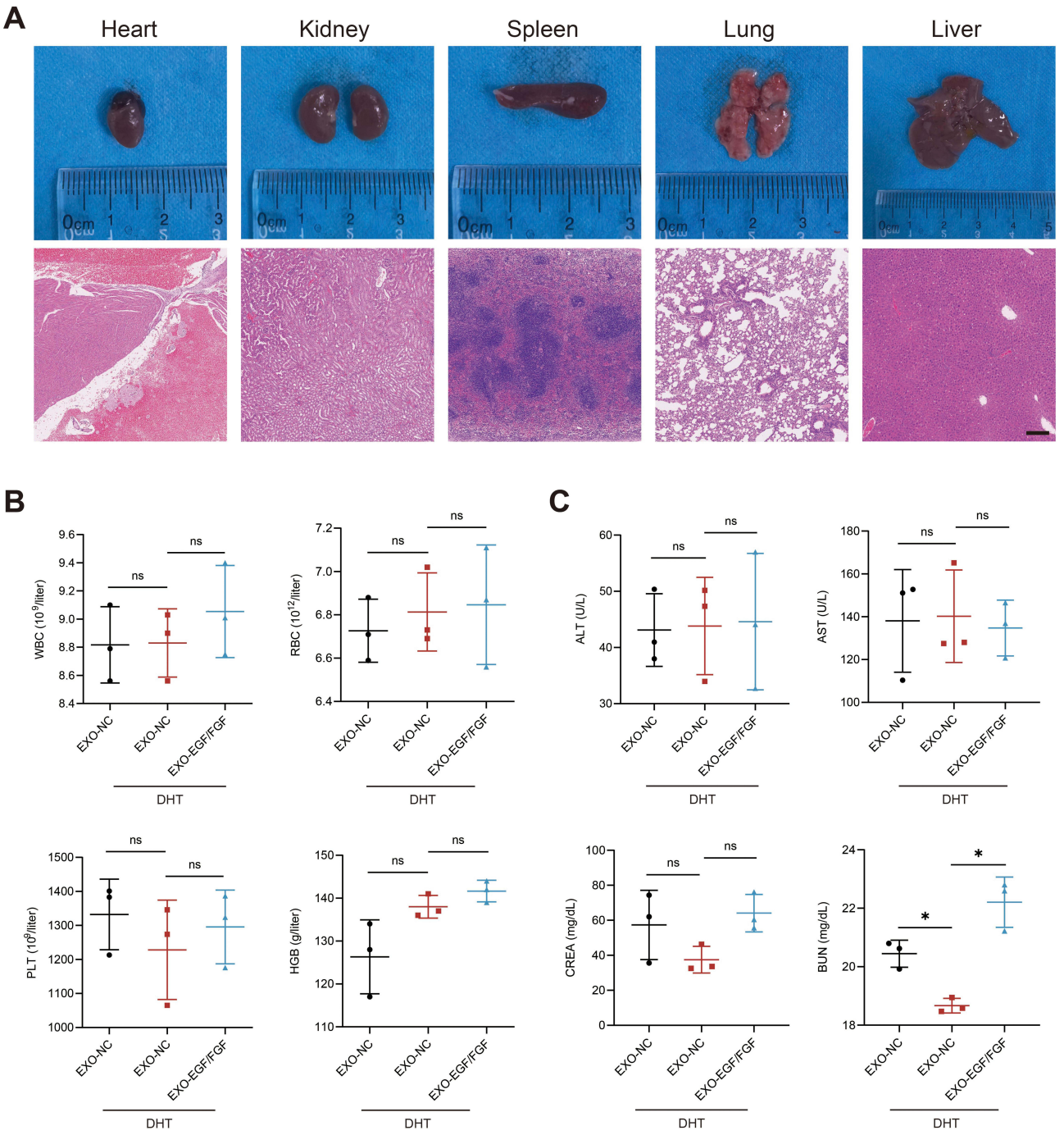

Figure 5 EXO-EGF/FGF exhibited in vivo safety. (**A**) HE-stained sections of major organs showed no toxicological damage. Scale bar = 200 μm. (**B**) Complete blood count parameters confirmed absence of abnormalities across all groups. (**C**) Hepatic and renal function indicators demonstrated no significant differences between the EXO-EGF /FGF-treated group and control groups. Ns = no significance.

designed a LAMP2B-EGF/FGF fusion protein targeted to the membrane surface of exosomes derived from 293T cells, creating engineered dual-factor exosomes overexpressing both EGF and FGF. Subsequently, we established both cellular and animal models of AGA to evaluate their therapeutic efficacy.

Conventional growth factor therapies faced two major challenges. On the one hand, free factors were susceptible to protease degradation in the interstitial space, exhibiting extremely short half-lives.[35] On the other hand, natural exosomes had limited loading capacity for growth factors, making it difficult to sustainably activate regenerative pathways.[36] For

instance, while exosomes held potential for treating ischemic stroke, they suffered from short half-lives, poor targeting specificity, and low concentrations at target sites.[37]

The engineered exosome design in this study demonstrates distinct advantages. By employing LAMP2B fusion expression technology (Figure 2A and B), EGF/FGF was precisely anchored onto the exosomal membrane, preventing degradation of free factors in the interstitial tissue. Subsequent in vitro experiments revealed that EXO-EGF/FGF exerts dual pro-regenerative effects on HFDPCs.

First, EXO-EGF/FGF promotes hair regeneration by restarting the growth cycle of AGA follicles. It effectively transitions HFDPCs in AGA follicles from a quiescent state (G0/G1) to a proliferative state (S phase) and upregulates the expression of the proliferation marker Ki67 (Figure 3A and B).

Second, EXO-EGF/FGF enhances hair regeneration by facilitating the migration of HFDPCs during the anagen initiation phase, thereby promoting critical dermal papilla-epithelial cell interactions (Figure 3C). After 48 hours of treatment with EXO-EGF/FGF, AGA-HFDPCs achieved a relative migration rate of 65.6%, significantly higher than the 35.8% observed in the AGA model group.

The therapeutic efficacy of EXO-EGF/FGF was further validated in AGA animal model induced by testosterone (Figure 4A). Experimental results demonstrated that subcutaneous injection of EXO-EGF/FGF significantly enhanced hair regeneration (Figure 4B). Within the treatment period, EXO-EGF/FGF treatment increased the hair coverage rate in AGA-affected areas from 21.5% to 58.4% (Figure 4C). Histological analysis via H&E staining confirmed the capacity of EXO-EGF/FGF to reverse miniaturized follicles into anagen-phase follicles, accompanied by characteristic morphological restoration (Figure 4D). Immunohistochemical findings further revealed the successful normalization of Ki67, EGF, and FGF expression levels in cutaneous follicles (Figure 4E). Notably, the lipid bilayer structure of EXO-EGF/FGF effectively shielded the immunogenicity of the encapsulated growth factors, with no detectable antibody production or allergic reactions observed in treated subjects, indicating exceptional tissue compatibility, hematological safety, and metabolic safety profiles (Figure 5).

A critical consideration for translating these preclinical findings to clinical practice is the difference in treatment timing and disease progression between the mouse model and human AGA patients. Our testosterone-induced mouse model develops AGA-like phenotypes within 4–6 weeks, whereas most clinical AGA patients present with a chronic disease course. Long-standing AGA involves more severe pathological alterations than the acute mouse model, including perifollicular fibrosis, chronic low-grade inflammation, and partial depletion of follicular stem cells.[38] Recent studies have indicated that perifollicular fibrosis in long-term AGA can block the interaction between DPCs and epithelial cells, thereby reducing follicular responsiveness to growth factor therapies.[39] This suggested that the efficacy of EXO-EGF/FGF may differ among patients with varying disease durations. It may be more effective in early-stage AGA, while for long-standing AGA, combination with anti-fibrotic or anti-inflammatory treatments might be necessary. Future clinical trials should stratify patients based on disease duration and optimize treatment regimens.

To further optimize this therapeutic platform, we propose two future directions, both of which are supported by recent advances in AGA research. First, alternative cell sources will be explored by replacing 293T cells with mesenchymal stromal cells, leveraging their innate secretion of immunomodulatory factors (such as TGF-β1 and IL-10) and pro-angiogenic factors (such as VEGF and HGF) to concurrently neutralize inflammatory signals in the AGA follicular microenvironment and stimulate perifollicular vascular reconstruction.[40] Second, formulation innovations will be pursued through the development of microneedle patches designed to replace conventional subcutaneous injections, thereby enabling painless self-administration while significantly enhancing bioavailability.[41]

Conclusion

In conclusion, this study developed and validated an engineered exosome-based strategy EXO-EGF/FGF utilizing LAMP2B membrane-anchoring technology for the treatment of AGA. This approach effectively overcame the critical limitations of conventional growth factor therapies, namely poor stability and lack of targeting, by achieving efficient and sustained delivery of EGF and FGF to the follicular microenvironment. The results demonstrated that EXO-EGF/FGF potently reactivates the hair growth cycle by stimulating the proliferation and migration of HFDPCs. In a testosterone-induced AGA animal model, the treatment significantly reversed follicular miniaturization and increased hair coverage.

Furthermore, EXO-EGF/FGF exhibited excellent biocompatibility and safety with no detectable immunogenicity. This study provided a novel, effective, and safe therapeutic strategy for functional hair regeneration, holding significant promise for clinical translation.

Data Sharing Statement

The datasets generated and analyzed during this study are available from the primary corresponding author, Professor Xiaofeng Ding, upon reasonable request.

Ethics Approval

All animal experimental protocols were approved by the Laboratory Animal Ethics Committee of Shanghai Skin Disease Hospital (Approval No. 2024-21) and were conducted in accordance with the National Institutes of Health Guide for the Care and Use of Laboratory Animals.

Consent for Publication

All authors consent to the publication of publication.

Author Contributions

Yongxian Lai and Junchao Wu should be considered as equal first co-authors. All authors made a significant contribution to the work reported, whether that is in the conception, study design, execution, acquisition of data, analysis and interpretation, or in all these areas; took part in drafting, revising or critically reviewing the article; gave final approval of the version to be published; have agreed on the journal to which the article has been submitted; and agree to be accountable for all aspects of the work.

Funding

This work was financially supported by the Clinical Research Incubation Project, Shanghai Skin Disease Hospital (LCFY-2022-06, LCFY-2021-05), Shanghai Qingpu District Health Commission Scientific Research Project (QWJ2024-37), Shanghai Science and Technology Innovation Action Plan Morning Star Project (24YF2738300), Peak Disciplines (Type IV) of Institutions of Higher Learning in Shanghai (GFFYKT06), Tongji University Medicine-X Interdisciplinary Research Initiative (2025-0650-YB-15).

Disclosure

The authors declare no conflicts of interest.

References

1. McElwee KJ, Sundberg JP. Innovative strategies for the discovery of new drugs against androgenetic alopecia. *Expert Opin Drug Discov*. 2025;20(4):517–536. doi:10.1080/17460441.2025.2473905
2. Inui S, Itami S. Molecular basis of androgenetic alopecia: from androgen to paracrine mediators through dermal papilla. *J Dermatol Sci*. 2011;61(1):1–6. doi:10.1016/j.jdermsci.2010.10.015
3. Krupa Shankar D, Chakravarthi M, Shilpakar R. Male androgenetic alopecia: population-based study in 1005 subjects. *Int J Trichol*. 2009;1(2):131–133. doi:10.4103/0974-7753.58556
4. Wang TL, Zhou C, Shen YW, et al. Prevalence of androgenetic alopecia in China: a community-based study in six cities. *Br J Dermatol*. 2010;162(4):843–847. doi:10.1111/j.1365-2133.2010.09640.x
5. Xiao Y, Zhang Y, Deng S, Yang X, Yao X. Immune and non-immune interactions in the pathogenesis of androgenetic alopecia. *Clin Rev Allergy Immunol*. 2025;68(1):22. doi:10.1007/s12016-025-09034-5
6. Olsen EA, Sinclair R, Hordinsky M, et al. Summation and recommendations for the safe and effective use of topical and oral minoxidil. *J Am Acad Dermatol*. 2025;93(2):457–465. doi:10.1016/j.jaad.2025.04.016
7. Mysore V. Finasteride and sexual side effects. *Indian Dermatol Online J*. 2012;3(1):62–65. doi:10.4103/2229-5178.93496
8. Avci P, Gupta GK, Clark J, Wikonkal N, Hamblin MR. Low-level laser (light) therapy (LLLT) for treatment of hair loss. *Lasers Surg Med*. 2014;46(2):144–151. doi:10.1002/lsm.22170
9. Queen D, Avram MR. Hair transplantation: state of the art. *Dermatol Surg*. 2025;51(9):874–881. doi:10.1097/DSS.0000000000004675
10. Zhou Y, Liu Q, Bai Y, et al. Autologous activated platelet-rich plasma in hair growth: a pilot study in male androgenetic alopecia with in vitro bioactivity investigation. *J Cosmet Dermatol*. 2021;20(4):1221–1230. doi:10.1111/jocd.13709

11. Gay D, Kwon O, Zhang Z, et al. Fgf9 from dermal gammadelta T cells induces hair follicle neogenesis after wounding. *Nat Med*. 2013;19(7):916–923. doi:10.1038/nm.3181
12. Wang X, Liu Y, He J, Wang J, Chen X, Yang R. Regulation of signaling pathways in hair follicle stem cells. *Burns Trauma*. 2022;10:tkac022. doi:10.1093/burnst/tkac022
13. Aguirre A, Rubio ME, Gallo V. Notch and EGFR pathway interaction regulates neural stem cell number and self-renewal. *Nature*. 2010;467(7313):323–327. doi:10.1038/nature09347
14. Zhang H, Nan W, Wang S, et al. Epidermal growth factor promotes proliferation of dermal papilla cells via Notch signaling pathway. *Biochimie*. 2016;127:10–18. doi:10.1016/j.biochi.2016.04.015
15. Yoo S, Kim J, Jeong ET, Hwang SJ, Kang NG, Lee J. Penetration rates into the stratum corneum layer: a novel quantitative indicator for assessing skin barrier function. *Skin Res Technol*. 2024;30(3):e13655. doi:10.1111/srt.13655
16. Shi M, McHugh KJ. Strategies for overcoming protein and peptide instability in biodegradable drug delivery systems. *Adv Drug Deliv Rev*. 2023;199:114904. doi:10.1016/j.addr.2023.114904
17. Zhao Z, Ukidve A, Kim J, Mitragotri S. Targeting strategies for tissue-specific drug delivery. *Cell*. 2020;181(1):151–167. doi:10.1016/j.cell.2020.02.001
18. Sadeghi S, Tehrani FR, Tahmasebi S, Shafiee A, Hashemi SM. Exosome engineering in cell therapy and drug delivery. *Inflammopharmacology*. 2023;31(1):145–169. doi:10.1007/s10787-022-01115-7
19. Inan Yuksel E, Cicek D, Demir B, et al. Garlic exosomes promote hair growth through the wnt/beta-catenin pathway and growth factors. *Cureus*. 2023;15(7):e42142. doi:10.7759/cureus.42142
20. Fu Y, Han YT, Xie JL, et al. Mesenchymal stem cell exosomes enhance the development of hair follicle to ameliorate androgenetic alopecia. *World J Stem Cells*. 2025;17(3):102088. doi:10.4252/wjsc.v17.i3.102088
21. Wang L, Huang Y, Wu Y, et al. Platelet-derived extracellular vesicles promote hair follicle growth through beta-catenin signaling pathway. *Platelets*. 2025;36(1):2498353. doi:10.1080/09537104.2025.2498353
22. Deng S, Cao H, Cui X, Fan Y, Wang Q, Zhang X. Optimization of exosome-based cell-free strategies to enhance endogenous cell functions in tissue regeneration. *Acta Biomater*. 2023;171:68–84. doi:10.1016/j.actbio.2023.09.023
23. He J, Ren W, Wang W, et al. Exosomal targeting and its potential clinical application. *Drug Deliv Transl Res*. 2022;12(10):2385–2402. doi:10.1007/s13346-021-01087-1
24. Li J, Zhao B, Dai Y, Zhang X, Chen Y, Wu X. Exosomes derived from dermal papilla cells mediate hair follicle stem cell proliferation through the wnt3a/beta-catenin signaling pathway. *Oxid Med Cell Longev*. 2022;2022:9042345. doi:10.1155/2022/9042345
25. Lin Y, Lu Y, Li X. Biological characteristics of exosomes and genetically engineered exosomes for the targeted delivery of therapeutic agents. *J Drug Target*. 2020;28(2):129–141. doi:10.1080/1061186X.2019.1641508
26. Li L, Wang F, Zhu D, Hu S, Cheng K, Li Z. Engineering exosomes and exosome-like nanovesicles for improving tissue targeting and retention. *Fundam Res*. 2025;5(2):851–867. doi:10.1016/j.fmre.2024.03.025
27. Wu X, Huang X, Zhu Q, et al. Hybrid hair follicle stem cell extracellular vesicles co-delivering finasteride and gold nanoparticles for androgenetic alopecia treatment. *J Control Release*. 2024;373:652–666. doi:10.1016/j.jconrel.2024.07.066
28. Aubin-Houzelstein G. Notch signaling and the developing hair follicle. *Adv Exp Med Biol*. 2012;727:142–160. doi:10.1007/978-1-4614-0899-4_11
29. Hu XM, Li ZX, Zhang DY, et al. A systematic summary of survival and death signalling during the life of hair follicle stem cells. *Stem Cell Res Ther*. 2021;12(1):453. doi:10.1186/s13287-021-02527-y
30. Kopan R, Ilagan MX. The canonical Notch signaling pathway: unfolding the activation mechanism. *Cell*. 2009;137(2):216–233. doi:10.1016/j.cell.2009.03.045
31. Xing H, Peng H, Yang Y, et al. Nitric oxide synergizes minoxidil delivered by transdermal hyaluronic acid liposomes for multimodal androgenetic-alopecia therapy. *Bioact Mater*. 2024;32:190–205. doi:10.1016/j.bioactmat.2023.09.021
32. Diviccaro S, Melcangi RC, Giatti S. Post-finasteride syndrome: an emerging clinical problem. *Neurobiol Stress*. 2020;12:100209. doi:10.1016/j.ynstr.2019.100209
33. Ma Y, Zhao J, Ning Y, et al. Dual-phase release finasteride-loaded microspheres for androgenetic alopecia treatment: rapid intervention and sustained control of dihydrotestosterone. *Int J Pharm*. 2025;683:126068. doi:10.1016/j.ijpharm.2025.126068
34. Legiawati L, Sitohang IBS, Yusharyahya SN, et al. Hair regeneration in androgenetic alopecia using secretome of adipose-derived stem cells (ADSC) and minoxidil: a comparative study of three groups. *Arch Dermatol Res*. 2025;317(1):486. doi:10.1007/s00403-025-04006-3
35. Varkhede N, Bommana R, Schoneich C, Forrest ML. Proteolysis and oxidation of therapeutic proteins after intradermal or subcutaneous administration. *J Pharm Sci*. 2020;109(1):191–205. doi:10.1016/j.xphs.2019.08.005
36. Wang J, Chen D, Ho EA. Challenges in the development and establishment of exosome-based drug delivery systems. *J Control Release*. 2021;329:894–906. doi:10.1016/j.jconrel.2020.10.020
37. Khan H, Pan JJ, Li Y, Zhang Z, Yang GY. Native and Bioengineered Exosomes for Ischemic Stroke Therapy. *Front Cell Dev Biol*. 2021;9:619565. doi:10.3389/fcell.2021.619565
38. Chen S, Li L, Ding W, Zhu Y, Zhou N. Androgenetic alopecia: an update on pathogenesis and pharmacological treatment. *Drug Des Devel Ther*. 2025;19:7349–7363. doi:10.2147/DDDT.S542000
39. Zhou S, Li Z, Li X, et al. Crosstalk between endothelial cells and dermal papilla entails hair regeneration and angiogenesis during aging. *J Adv Res*. 2025;70:339–353. doi:10.1016/j.jare.2024.05.006
40. Trigo CM, Rodrigues JS, Camoes SP, Sola S, Miranda JP. Mesenchymal stem cell secretome for regenerative medicine: where do we stand? *J Adv Res*. 2025;70:103–124. doi:10.1016/j.jare.2024.05.004
41. Jing S, Liu Y, Wang B, et al. Microneedle-mediated hypoxic extracellular vesicle-encapsulated selenium nanoparticles delivery to treat androgenetic alopecia. *J Control Release*. 2025;381:113597. doi:10.1016/j.jconrel.2025.113597